Cement and Concrete Research 40 (2010) 1239–1247

Contents lists available at ScienceDirect

Cement and Concrete Research

journal homepage: http://ees.elsevier.com/CEMCON/default.asp

Hydration of calcium sulfoaluminate cements — Experimental findings and thermodynamic modelling

Frank Winnefeld *, Barbara Lothenbach

Empa, Swiss Federal Laboratories for Materials Testing and Research, Laboratory for Concrete and Construction Chemistry, Dübendorf, Switzerland

ARTICLE INFO

Article history:
Received 14 May 2009
Accepted 19 August 2009

Keywords:
Calcium sulfoaluminate cement
B. Hydration products
B. Pore solution
Thermodynamic modeling

ABSTRACT

Calcium sulfoaluminate cements (CSA) are a promising low-CO_2 alternative to ordinary Portland cements and are as well of interest concerning their use as binder for waste encapsulation. In this study, the hydration of two CSA cements has been investigated experimentally and by thermodynamic modelling between 1 h and 28 days at *w/c* ratios of 0.72 and 0.80, respectively.

The main hydration product of CSA is ettringite, which precipitates together with amorphous $Al(OH)_3$ until the calcium sulfate is consumed after around 1–2 days of hydration. Afterwards, monosulfate is formed. In the presence of belite, strätlingite occurs as an additional hydration product. The pore solution analysis reveals that strätlingite can bind a part of the potassium ions, which are released by the clinker minerals. The microstructure of both cements is quite dense even after 16 h of hydration, with not much pore space available at a sample age of 28 days.

The pore solution of both cements is dominated during the first hours of hydration by potassium, sodium, calcium, aluminium and sulfate; the pH is around 10–11. When the calcium sulfate is depleted, the sulfate concentration drops by a factor of 10. This increases pH to around 12.5–12.8.

Based on the experimental data, a thermodynamic hydration model for CSA cements based on cement composition, hydration kinetics of clinker phases and calculations of thermodynamic equilibria by geochemical speciation has been established. The modelled phase development with ongoing hydration agrees well with the experimental findings.

1. Introduction

Concrete, mainly based on Portland cement, is the most used material worldwide, with a production of about $1.7 \cdot 10^9$ t/year [1]. The production of Portland cement clinker accounts for about 5% of the total man-made CO_2-emissions, as the production of 1 t cement clinker generates about 800 kg of CO_2 [1,2]. There are several ways for a more environmental friendly cement production like blending Portland cement clinker with supplementary cementitious materials or the use of alternative fuels in the cement kiln.

Another way is changing the binder chemistry to a non-Portland cement based system. A promising low-CO_2 alternative is the production of clinkers based on calcium sulfoaluminate (ye'elimite, $C_4A_3\overline{S}$ [1]) [1–5]. They can be made from calcium sulfate, limestone and bauxite at a temperature of about 1250 °C [6,7]. Thus, the firing temperature is about 200 °C lower than for ordinary Portland cement clinker. Compared to alite (1.80 g CO_2/ml of the cementing phase), calcium sulfoaluminate releases only 0.56 g CO_2/ml cementing phase [1]. In addition, this type of clinker is easier to grind compared to ordinary Portland cement. Depending on the raw meal composition, calcium sulfoaluminate-based clinkers may contain various minor phases such as belite, calcium aluminate ferrate, excess anhydrite, gehlenite or mayenite [8]. Besides the raw materials mentioned above, various industrial by-products or waste materials like fly ash, blast furnace slag, phosphogypsum, baghouse dust or scrubber sludge can be used for the manufacturing of calcium sulfoaluminate-based clinkers [9–11].

Usually about 15–25 wt.% of gypsum is interground with the clinker for optimum setting time, strength development and volume stability [5]. The hydration of the calcium sulfoaluminate cements (CSA) obtained depends mainly on the amount and reactivity of the added calcium sulfate [12,13] as well as on the kind and amount of minor phases present. The water demand for complete hydration is determined by the amount of calcium sulfate added and is at a maximum around an addition of 30% [5]. The required water/cement ratio for complete hydration is higher compared to an OPC, e. g. 0.78 for pure ye'elimite reacting with 2 mol of anhydrite [14]. In comparison to ordinary Portland cement, cements based on calcium

* Corresponding author.
E-mail address: Frank.Winnefeld@empa.ch (F. Winnefeld).

[1] Cement notation: A = Al_2O_3, C = CaO, H = H_2O, S = SiO_2, $\overline{S}$ = SO_3.

0008-8846/$ – see front matter © 2009 Elsevier Ltd. All rights reserved.
doi:10.1016/j.cemconres.2009.08.014

sulfoaluminate react faster, and most of the hydration heat evolution occurs between 2 and 12 h of hydration [15]. As main crystalline hydration products ettringite and monosulfate are formed together with amorphous aluminium hydroxide (Eqs. (1) and (2)).

$$C_4A_3\overline{S} + 18H \rightarrow C_3A \cdot C\overline{S} \cdot 12H + 2AH_3 \text{(monosulfate formation)} \quad (1)$$

$$C_4A_3\overline{S} + 2C\overline{S}H_2 + 34H \rightarrow C_3A \cdot 3C\overline{S} \cdot 32H + 2AH_3 \text{(ettringite formation)} \quad (2)$$

Depending on the minor phases present in CSA cements, various other hydration products may occur such as C–S–H phases, strätlingite, monocarboaluminate, gibbsite or hydrogarnet [4,5,15–18].

Data on the pore solution composition of CSA cements is very scarce in literature. A complete data set at realistic water/cement ratios is reported in [16], where the pore solution chemistry of a CSA clinker was determined at hydration times from 1 to 60 days at water/cement ratios between 0.5 and 0.8. The authors found a rapid release of soluble alkalis from the clinker accompanied by a high pH around 13. Aluminium concentrations are generally higher compared to Portland cements, while sulfate concentration reached a maximum at a sample age of 7 days. Pore solution data of a calcium sulfoaluminate cement are given in [18], but determined at a high water cement/ratio of 20. The consumption of the calcium sulfate after about 8 h is indicated by a sharp drop of calcium and sulfate concentration and an increase of the aluminium concentration.

Microstructural investigations [15,17] revealed mainly the formation of large space filling ettringite needles, together with monosulfate, aluminium hydroxide and calcium silicate hydrates, leading to a very dense, low-porosity microstructure.

Compared to OPC, CSA cements reach higher early and late strengths [5]. Their strength development [13] and volume stability [19] depend on the kind and amount of the calcium sulfate added. Durability, e. g. sulfate and carbonation resistance [20,21], seems to be sufficient, as also shown by examination of existing structures made from CSA concrete [4,5,17]. Besides the use as binder for mortar or concretes, the main applications of calcium sulfoaluminate cements are on one hand as expansive compound in shrinkage-compensated cements or as addition to special concretes like high early strength concrete, self-levelling screeds or high-performance glass-fibre-reinforced composites [22–25]. On the other hand, due to their low pH, their low-porosity and the ability of ettringite and AFm phases to bind heavy metals, calcium sulfoaluminate cements are of interest in the field of hazardous waste encapsulation [26–30].

In order to understand better the hydration mechanisms of CSA cements, the composition and development of the solid and the liquid phase during hydration of two commercial products were determined in this study. The ionic composition of the liquid phase is linked to the precipitation of hydrates, which control the setting and hardening. Based on this analytical data, thermodynamic modelling of the interactions between solid and liquid phase is applied in order to improve the chemical understanding of hydration processes. For the modelling, GEMS-PSI, a geochemical speciation code [31], involving a thermodynamic database [32–34], which has been upgraded with cement-specific data by Lothenbach, Matschei, Glasser and co-workers [35–38], is used. Thermodynamic modelling has previously been applied to the hydration of Portland cement [35,39], Portland limestone cement [40] and of alkali and sulfate activated ground granulated blast furnace slags [41,42].

2. Materials

Two commercial CSA cements were investigated; their chemical analysis is given in Table 1. CSA-1 was produced in the laboratory by blending 78% of a commercial CSA clinker (density 2.78 g/cm^3, Blaine surface area 4860 cm^2/g) with 22% of calcium sulfate dihydrate (Fluka). CSA-2 (density 2.84 g/cm^3, Blaine surface area 4630 cm^2/g) was used as provided by the manufacturer. It included already the calcium sulfate, in this case anhydrite. CSA-1 contained more aluminium and less silica than CSA-2. Its main constituents derived from X-ray diffraction analysis and stochiometric calculations based on the XRF analysis were ye'elimite (50%), gehlenite (15%), calcium aluminate (8%) and gypsum (22%). CSA-2 consisted of ye'elimite (54%), belite (19%) and anhydrite (21%). Minor phases in both products were mainly titanium containing phases. Gehlenite and the titanium containing phases can be regarded as hydraulically inactive.

Table 1
Chemical composition of the used CSA cements (referred to cement as delivered).

	CaO wt.%	SiO_2 wt.%	Al_2O_3 wt.%	Fe_2O_3 wt.%	MgO wt.%	Na_2O wt.%	K_2O wt.%	TiO_2 wt.%	SO_3 wt.%	L.O.I. wt.%
CSA-1	34.4	3.2	35.5	0.88	0.76	0.05	0.21	1.8	16.8	5.1
CSA-2	41.2	6.9	26.8	0.88	0.75	0.13	0.40	1.2	19.5	1.8

L.O.I.: loss on ignition.

3. Methods

To investigate the hydration of the two cements, cement pastes were prepared with water/cement ratios of 0.72 (CSA-1) and 0.80 (CSA-2). All hydration experiments were carried out at 20 °C.

A conduction calorimeter (Thermometric TAM Air) was used to determine the rate of hydration heat liberation during the first 72 h. 6.00 g of cement were weighed into a flask and the corresponding amount of water was added. The mixing was done by a small stirrer for 1 min. The flask was then capped and placed into the calorimeter. Due to the external mixing, the very early thermal response of the samples could not be measured. The total heat of hydration after 72 h was determined by integration of the heat flow curve between 30 min and 72 h.

Hydration experiments to determine the composition of solid and liquid phases at various ages were carried out as follows: for hydration times up to 4 h, 50 g of cement and the mixing water were placed in a plastic container and mixed by hand with a spatula for 2 min. The plastic containers were sealed and stored at 20 °C. The pore solutions were gained by pressure filtration using a 0.45 µm Nylon filter. For longer hydration times (5 h and beyond), larger samples of 1000 g cement were mixed with water according to EN 196-3. The pastes were cast in 500 ml polyethylene bottles, sealed and stored at 20 °C. Those pore fluids were extracted using the steel die method [43] and immediately filtered using 0.45 µm Nylon filters.

For further analysis, one part of the solution was diluted by 1:4 with HNO_3 (6.5%) to prevent precipitation of solids and carbonation. The total concentrations of the elements were determined using inductively plasma optical emission spectroscopy (ICP-OES). The other part was used for pH measurements. The hydroxide concentrations were determined with a combined pH electrode on the filtered and undiluted solutions. The pH electrode was calibrated against KOH solutions of known concentrations.

The hydration of the solid phase was stopped by submerging a part of the crushed pastes in isopropanol, filtering and washing the residue first with isopropanol and then with diethyl ether. The samples were then stored for 3 days in a desiccator over silica gel.

In a comparative study, this technique was found to be suitable for this kind of samples. In addition, its reliability was cross-checked using slices cut from hardened pastes (age 16 h and beyond), which were measured by X-ray diffraction and thermogravimetric analysis without stopping hydration.

After stopping hydration, a part of the sample was ground by hand below 0.063 mm. Thermogravimetric analysis (TGA) was carried out in N_2 atmosphere on about 10 mg of sample using a Mettler-Toledo TGA/

SDTA 851 instrument at 20 °C/min up to 980 °C. The experimental data was compared with reference measurements on pure hydrate phases. Chemically bound water was determined as the weight loss at 600 °C. From this, the amount of pore solution can be back calculated. The amount of ettringite in the hydrated pastes was determined as described in [39], assuming that the weight loss between 50 °C and 120 °C corresponds to 20 molecules of crystal water, per molecule of ettringite. Gypsum content was calculated from the TGA weight loss between 120 and 150 °C.

X-ray diffraction (XRD) patterns were measured with a Panalytical X'pert Pro powder diffractometer equipped with an X'Celerator detector in a 2θ-range of 5–80°. The dissolution kinetics of $C_4A_3\overline{S}$, CA, C_2S and anhydrite were determined semiquantitatively from the intensities of the corresponding XRD reflections and corrected for the amount of bound water.

Unground pastes were examined by scanning electron microscopy (Philips ESEM FEG XL 30) using backscattered electron images and energy dispersive X-ray (EDS) analysis of polished surfaces. Sample preparation included pressure impregnation with epoxy resin, cutting, polishing and coating with carbon.

Thermodynamic modelling was carried out using the geochemical GEMS-PSI software [31], coupled with the cement-specific CEMDATA database [38]. As a first step, the pore solution composition was used to calculate the saturation indices of possible hydrate phases. This gives an indication of which hydrates are in equilibrium with the pore solution and thus might precipitate. If the pore solution is undersaturated with respect to a certain solid, this solid is not likely to precipitate. Based on the experimental data, a thermodynamic model of the hydration process of CSA cements was set up in the following steps: (i) The chemical composition of the cements was used as input data, (ii), the dissolution kinetics of the clinker phases $C_4A_3\overline{S}$, CA and C_2S as well as of anhydrite in the case of CSA-2 were taken from the X-ray diffraction patterns, whereas the more reactive gypsum was allowed to dissolve freely, and (iii) the thermodynamic equilibria for the solid phases involved were calculated by GEMS depending on the dissolution kinetics of the above mentioned solids.

4. Results and discussion

4.1. Isothermal calorimetry

The results of conduction calorimetry are given in Fig. 1. Cement CSA-1 has a dormant period after the initial peak until a sample age of about 4 h. The main hydration peak occurs at 7 h, with a shoulder after about 16 h. Sample CSA-2 also shows a dormant period until 4 h, followed by a first main hydration peak after 7 h. A second heat flow maximum occurs after 26 h of hydration. The total heat of hydration after 72 h is 377 J/g for CSA-1 and 392 J/g for CSA-2.

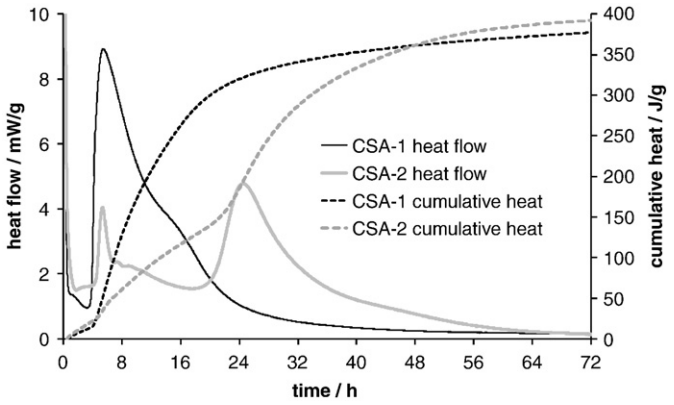

Fig. 1. Isothermal conduction calorimetry of the CSA cements.

4.2. X-ray diffraction and thermogravimetric analysis

The changes of the solid phase composition with ongoing hydration were determined by XRD and TGA. XRD analyses (Fig. 2) of CSA-1 reveal that even after 1 h of hydration a part of the $C_4A_3\overline{S}$, CA and gypsum have been consumed, and ettringite has formed as new crystalline phase. Between 1 h and 5 h of hydration just a slight progress of hydration is visible, whereas the hydration accelerates a lot between 5 h and 16 h as can be seen from the ye'elimite and gypsum consumption and from ettringite formation. After 16 h of hydration, traces of monosulfate are detectable, while gypsum has almost been depleted. Beyond 16 h the hydration kinetics slows down again, displaying only a slight increase of the amount of hydration products. After 28 days the crystalline phase assemblage of hydrated CSA-1 consists of the hydrate phases ettringite and monosulfate, as well as some non reacted traces of C_4A_3s, gypsum and the inert phases (mainly gehlenite). Crystalline $Al(OH)_3$ (gibbsite) is not detected, thus it can be assumed that it occurs in an X-ray amorphous form.

The XRD results are confirmed by the TGA data (Fig. 3). Contrary to the XRD data, $Al(OH)_3$ is detectable due to the water loss at around 300 °C. After 1 h of hydration ettringite (weight loss at 50 °C–120 °C) has formed together with some $Al(OH)_3$, consuming a part of the gypsum (weight loss at around 150 °C). Between 1 h and 2 h of hydration almost no increase of the amount of ettringite occurs. After 2 h and until 2 days the hydration continues with the consumption of the gypsum and formation of ettringite and $Al(OH)_3$. Afterwards, ettringite formation is mainly completed. After 16 h of hydration, monosulfate starts to form (weight loss at about 190 °C). Amorphous $Al(OH)_3$ forms during both in the ettringite dominated period of hydration (until 2 days) and in the monosulfate dominated (beyond 2 days) period of hydration.

The XRD analyses of hydrated CSA-2 (Fig. 4) reveal a similar phase development as for CSA-1. Anhydrite and $C_4A_3\overline{S}$ are consumed, and ettringite forms during the first. Gypsum is never detected by XRD, as any sulfate originating from the dissolution of anhydrite is rapidly consumed by the formation of ettringite. The dissolution kinetics of the anhydrite used in CSA-2 seems to be slower than that of the gypsum present in CSA-1. A similar effect is described in [12,13], where the readily soluble dihydrate promotes a rapid ettringite formation, whereas anhydrite causes a delay in early ettringite precipitation, resulting in poor early strength. From hydration times of 2 days on also traces of monosulfate can be detected. At that time the formation of ettringite has terminated. After 28 days, strätlingite, C_2ASH_8, has formed from belite as silicon source and $C_4A_3\overline{S}$ and/or AH_3 as aluminium source in agreement with [18] and according to Eq. (3).

$$C_2S + AH_3 + 5H \rightarrow C_2ASH_8 \text{ (strätlingite formation)}$$

Strätlingite is only stable in the absence of portlandite [44]. Other phases present at 28 days are unhydrated $C_4A_3\overline{S}$ and anhydrite as well as ettringite and traces of monosulfate.

TGA results (Fig. 5) reveal an increase of ettringite quantity until 2 days of hydration. Afterwards, the ettringite content stays rather constant. Traces of monosulfate are detectable after 2 days of hydration. Al$(OH)_3$ forms continuously as additional hydration product. In contrast to CSA-1, CSA-2 shows almost no increase of $Al(OH)_3$ beyond the hydration time of 2 days. This can be explained by the fact that $Al(OH)_3$ is consumed by the formation of strätlingite, as the belite present in CSA-2 starts to take part in the hydration processes after several days. The strätlingite formed can be identified in the sample hydrated for 28 days (weight loss at 160 °C) besides ettringite, $Al(OH)_3$ and traces of monosulfate.

4.3. Scanning electron microscopy

CSA-1 already has a quite dense microstructure after 16 h of hydration, see Fig. 6 (a). Besides unhydrated clinker grains and non reacted, plate-like gypsum crystals, ettringite crystals of about 10 µm

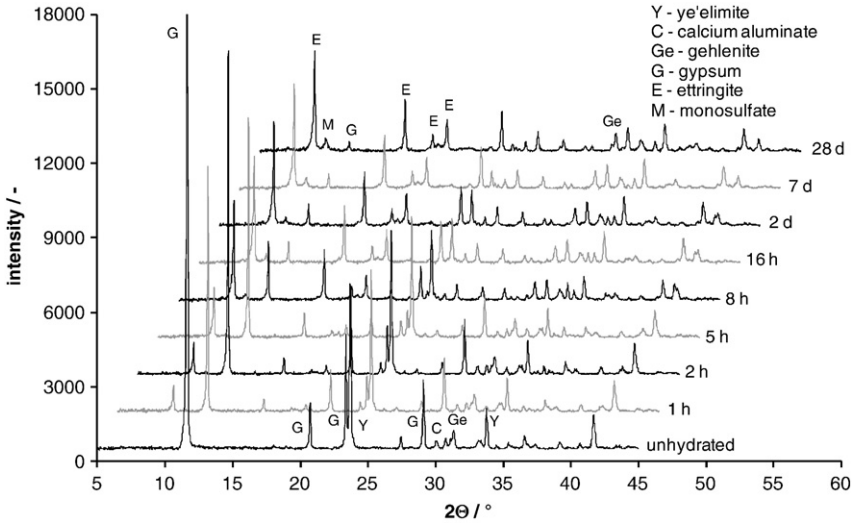

Fig. 2. X-ray diffraction analysis of CSA-1; unhydrated sample and after 1. 2, 5, 8, 16 h, 2, 7, 28 days of hydration at $w/c = 0.72$.

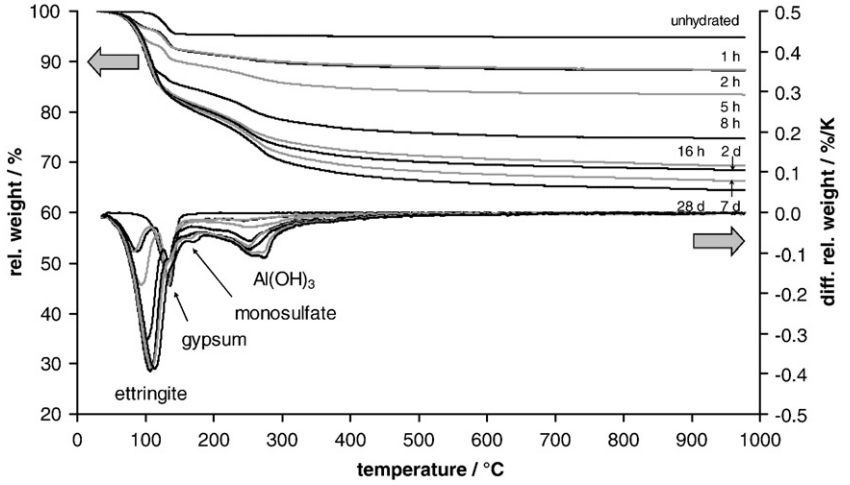

Fig. 3. Thermogravimetric analysis of CSA-1; unhydrated sample and after 1. 2, 5, 8, 16 h, 2, 7, 28 days of hydration at $w/c = 0.72$.

size and areas exhibiting a dark grey level consisting mainly of aluminium hydroxide can be identified with the help of EDX analyses. After 28 days of hydration, see Fig. 6 (b), only a few clinker relics occur in the very dense microstructure of hydrated CSA-1. The inert iron and titanium containing phases are very well visible due to their high brightness in the backscattered electron image.

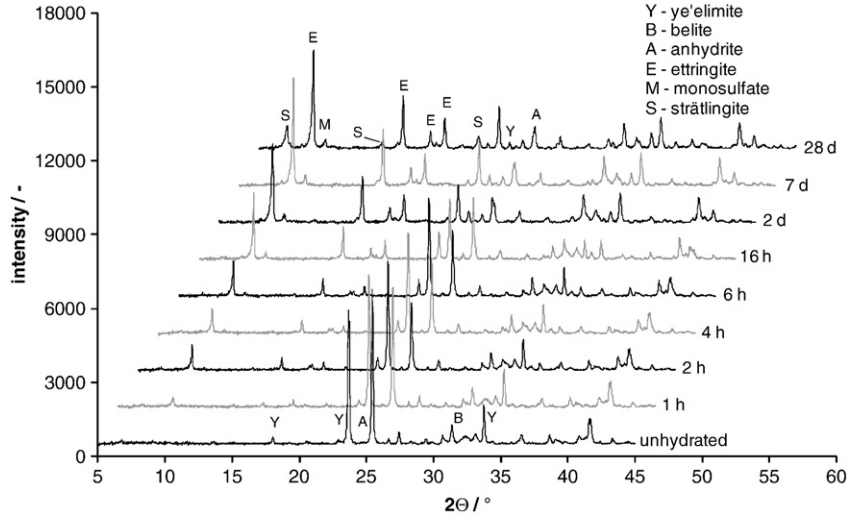

Fig. 4. X-ray diffraction analysis of CSA-2; unhydrated sample and after 1, 2, 4, 6, 16 h, 2, 7, 28 days of hydration at $w/c = 0.80$.

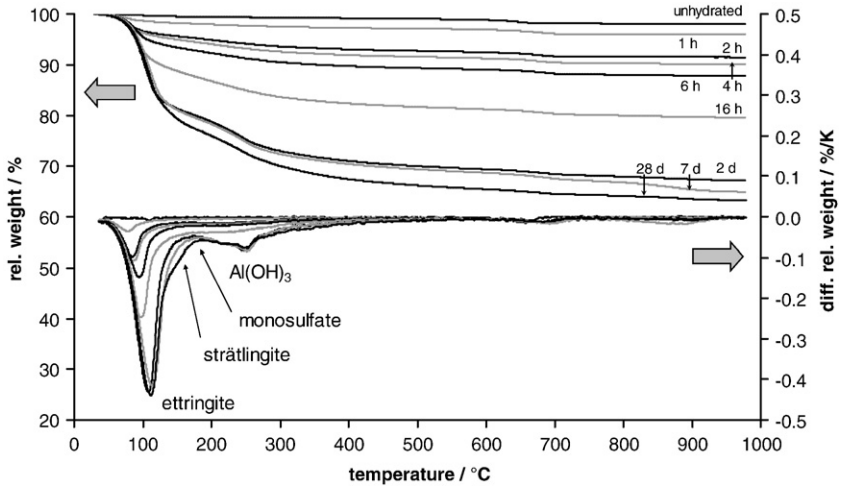

Fig. 5. Thermogravimetric analysis of CSA-2; unhydrated sample and after 1, 2, 4, 6, 16 h, 2, 7, 28 days of hydration at $w/c = 0.80$.

Fig. 6 (c) displays the microstructure of hydrated CSA-2 after 16 h of hydration. It is quite dense as well, however there tend to be more unhydrated clinker particles present compared to CSA-1 at the same sample age. As hydration products ettringite crystals and $Al(OH)_3$ (areas with a dark grey level) can be recognized. After 28 days of hydration, see Fig. 6 (d), still some clinker relicts occur. Besides ettringite and $Al(OH)_3$, plate-like crystals can be recognized, which could be identified as strätlingite by EDX analysis.

When comparing the SEM images of both cement pastes, the microstructure of CSA-1 appears much more homogeneous than the one of CSA-2. This is true for the samples after 16 h of hydration and especially for the samples at 28 days due to the large amounts of strätlingite formed in CSA-2.

4.4. Pore solution chemistry

The composition of the pore solution of CSA-1 and CSA-2 is shown in Table 2.

During the first hours of hydration the pore solution chemistry of CSA-1 is dominated by alkali, calcium, aluminium and sulfate (ICP-OES used here to determine pore solution composition is an elemental analysis; strictly speaking sulfur is determined instead of sulfate). The pH values are quite low (pH 10.3–10.7) compared to a Portland cement (pH 13–14). As hydration proceeds, the alkali ion concentration in the pore solution increases due to the continuous release of Na and K by dissolution of the reactive anhydrous phases, whereas Ca and sulfate concentrations are buffered by the gypsum. After 16 h of

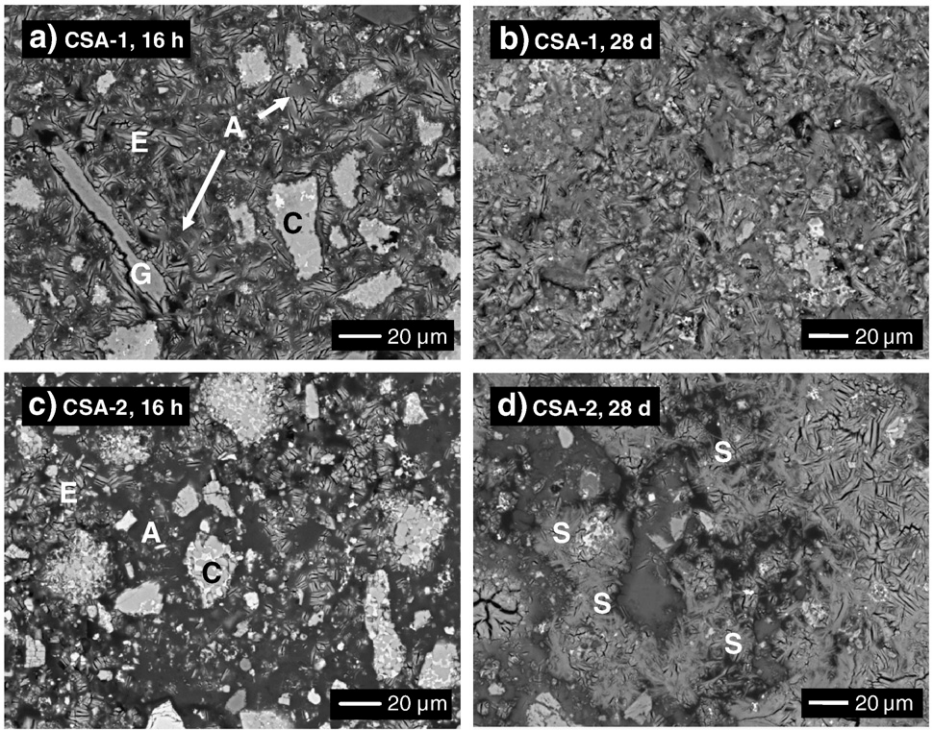

Fig. 6. SEM images of CSA-1 hydrated for 16 h (a) and for 28 days (b), and of CSA-2 hydrated for 16 h (c) and for 28 days (d) C = CSA clinker, G = gypsum, E = ettringite, A = aluminium hydroxide, S = strätlingite.

Table 2
Pore solution chemistry of the CSA cements.

Time 0	Na mmol/l	K mmol/l	Ca mmol/l	Al mmol/l	Si mmol/l	S mmol/l	OH mmol/l	pH
CSA-1								
1 h	0.60	2.1	18	10	<0.01	19	0.50	10.7
2 h	0.77	2.8	17	9.9	<0.01	19	0.38	10.6
5 h	3.0	9.2	15	7.3	0.01	21	0.19	10.3
8 h	7.8	29	13	7.5	0.02	31	0.19	10.3
16 h	16	59	1.2	51	0.02	19	6.6	11.8
2 days	16	98	0.60	100	0.03	1.9	27	12.4
7 days	17	120	0.57	120	0.04	2.1	43	12.6
28 days	21	120	0.31	100	0.05	3.4	50	12.7
CSA-2								
1 h	11	52	11	20	<0.01	36	0.73	10.9
2 h	14	60	4.4	51	0.01	20	2.1	11.3
4 h	15	62	4.3	47	0.01	22	1.8	11.2
6 h	15	65	3.4	52	0.01	21	1.5	11.2
16 h	16	65	3.0	59	0.01	18	2.7	11.4
2 days	41	140	0.41	101	0.09	32	16	12.2
7 days	44	140	0.42	91	0.18	11	73	12.9
28 days	34	82	0.23	26	0.21	9	70	12.8
Detection limit								
	0.002	0.001	0.001	0.004	0.01	0.005	–	–

hydration a remarkable change in the pore solution chemistry occurs. Due to the depletion of gypsum, sulfate and calcium concentrations decrease by a factor of 10. As electroneutrality of the pore solution has to be maintained, hydroxide concentration increases, leading to a pH value of 11.8. With the depletion of gypsum and the pH increase the aluminium concentration increases strongly. After 28 days of hydration, the pH value has further increased to a value of 12.7. This is caused by the ongoing release of alkali ions from the CSA clinker and by the continuous consumption of the pore fluid by the formation of hydrates, which increases the alkali concentrations as well. The silicon concentrations are generally in the range of 0.01–0.05 mmol/l and increase with increasing pH of the pore solution.

For CSA-2, in general follows similar trends to CSA-1, but CSA-2 displays higher concentrations for most of the elements measured. Especially alkali, hydroxide and at early ages aluminium concentrations are much higher, yielding a higher pH in the pore solution compared to CSA-1 during the first hours of hydration (10.9 after 1 h, and 11.2 after 6 h). Calcium concentrations at these sample ages are lower compared to CSA-1, probably caused due to the higher Al concentrations.

After 2 days of hydration, the calcium concentration has decreased strongly, whereas sulfate concentrations show a decrease at 7 days of hydration. Aluminium, sodium and potassium concentrations show a maximum at a sample age of 2 days, while at later ages a decrease is observed. The decrease in sodium and especially potassium concentration, especially of K, indicates an uptake of these ions by one (or more) of the occurring hydration products, which is in agreement with the pore solution data obtained by Andac and Glasser [16]. As strätlingite forms mainly between 7 and 28 days of hydration, it is very likely that strätlingite can act as a sink for potassium ions.

CSA-2 shows at all hydration times slightly higher pH values than CSA-1. During the first hours of hydration, the pH is around 10.9–11.3, whereas at 28 days a pH of 12.8 was measured. For both cements, the drop in sulfate and Ca concentration between 16 h and 2 days coincidences with the heat flow measurements, where a shoulder after 16 h (CSA-1) and a maximum after 26 h (CSA-2) is observed.

Li et al. [18] analysed the liquid phase of a sulfoaluminate belite cement suspension at a water/cement ratio of 20 up to a hydration time of 24 h. Their results show for Ca and sulfate similar concentrations, and for all elements similar trends as our measurements, i.e. the continuing release of alkalis and the sharp drop of calcium and sulfate concentrations, indicating the consumption of the anhydrite. Andac and Glasser [16] determined the pore solution chemistry of a calcium sulfoaluminate clinker containing belite a minor hydraulic phase, hydrated between 1 and 60 days at a water/cement ratio of 0.80. Compared to CSA-2, which is a product of similar composition, but with additional anhydrite added, Andac and Glasser found somewhat different values, especially a much higher pH at the first days of hydration. Their alkali concentrations are in the same order compared to CSA-2, whereas their values for Ca, Al and S are lower.

4.5. Thermodynamic modelling

4.5.1. Saturation indices

As a first step the analytical data of the pore solutions of CSA-1 and CSA-2 was taken to calculate the saturation indices with respect to possible hydrate phases in order to reveal which phases could precipitate. The saturation index with respect to a certain solid phase is calculated as $\log(IAP/K_{S0})$. The ion activity product IAP is calculated from the concentrations determined in the pore solution, while K_{S0} is the solubility product under equilibrium conditions. As the use of saturation indices can be misleading when comparing phases which dissociate into a different number of ions, "effective" saturation indices were calculated by dividing the saturation indices by the number of ions participating in the reactions to form the solids. The formation from the dominant ions OH^-, H^+, Ca^{2+}, SO_4^{2-}, $SiO(OH)_3^-$ or $Al(OH)_4^-$ in the solution was considered while the influence of H_2O was ignored. The values for gypsum/anhydrite, $Al(OH)_3$, CAH_{10}, tobermorite, portlandite, strätlingite, monosulfate or ettringite were divided by 2, 2, 2.5, 3, 3, 6, 11, or 15 respectively. Note that a high saturation index does not correlate with a high amount of the respective solid present in the system.

Fig. 7 shows the data for selected hydrates. In CSA-1, ettringite is always highly oversaturated; the degree of oversaturation decreases a bit with time, especially when the gypsum is consumed. Amorphous $Al(OH)_3$ is always slightly oversaturated. The pore solution is saturated with respect to gypsum until a sample age of 8 h; from 16 h on, gypsum is undersaturated. Monosulfate on the contrary is undersaturated until 8 h, afterwards it becomes oversaturated. This behaviour of gypsum and monosulfate is in agreement with data of the solid phase composition. Strätlingite is always oversaturated, whereas C–S–H phases (tobermorite and jennite) are undersaturated. This indicates that C–S–H phases should not be present, but the Si concentration in the pore solution is instead controlled by strätlingite. Portlandite is always undersaturated and thus should not precipitate either. Regarding the possible calcium aluminate hydrates, CAH_{10} is the only oversaturated phase. However, not every phase, which is calculated to be oversaturated, will precipitate, depending on the kinetic of precipitation and whether any other phase is thermodynamically even more stable.

In cement CSA-2, ettringite is always oversaturated. Unlike in CSA-1, gypsum is saturated in CSA-2 pore solutions only in the first hour of hydration, afterwards it becomes undersaturated. This reflects the slower dissolution kinetics of the anhydrite compared to the gypsum in CSA-1, leading to a depletion of available calcium and sulfate in the pore solution due to rapid ettringite formation. Monosulfate is oversaturated throughout the whole investigated hydration period. As in CSA-1, strätlingite is always oversaturated, and C–S–H phases are always undersaturated. Thus, the formation of C–S–H is not likely to occur in this cement, despite the belite content of 19%. Portlandite is also always undersaturated. Amorphous $Al(OH)_3$ is oversaturated until a hydration time of 7 days. At 28 days it is found to be undersaturated, which indicates its (partial) consumption by the formation of strätlingite. For CAH_{10} similar saturation indices occur as in CSA-1, but the phase could not be identified in CSA-2 either.

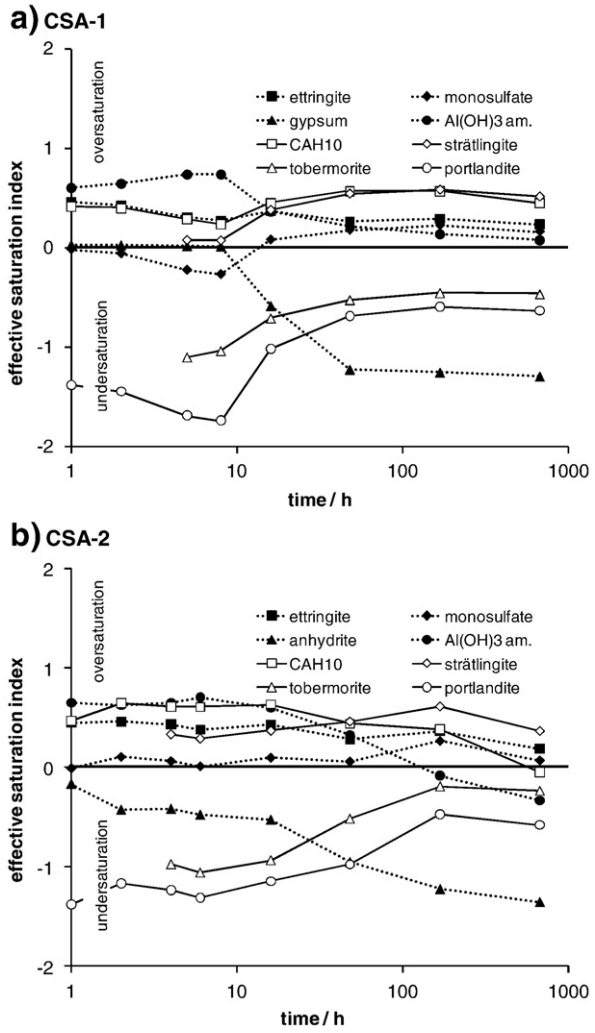

Fig. 7. Effective saturation indices calculated from the pore solution chemistry of a) CSA-1 and b) CSA-2 (lines for eye guide only).

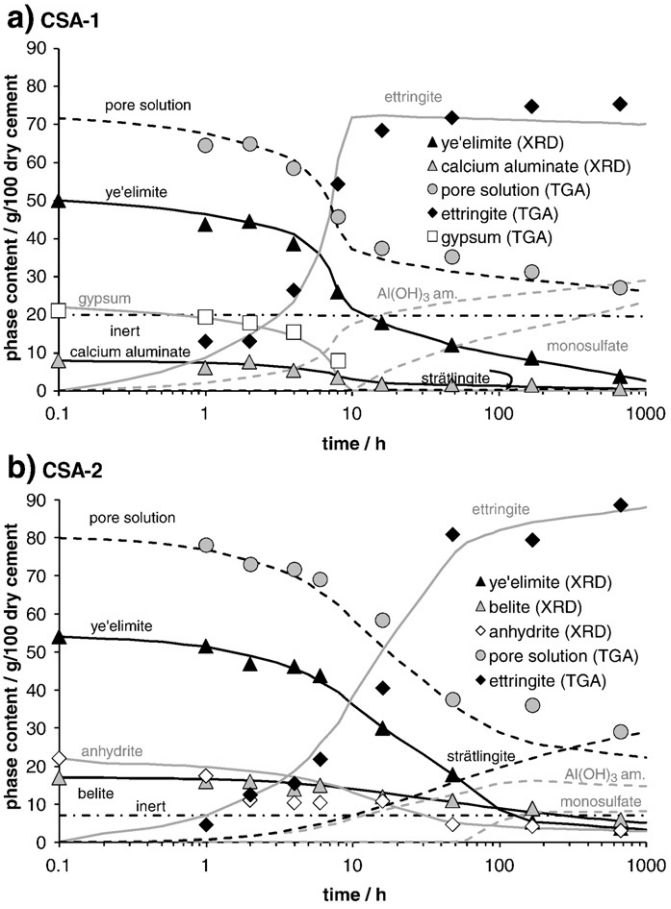

Fig. 8. Modelled evolution of solid phases and pore solution quantity during hydration of a) CSA-1 and b) CSA-2; data points: experimental data.

4.5.2. Modelling of hydration

A thermodynamic model of the hydration of CSA-1 and CSA-2 pastes was set up, based on the empirical dissolution kinetics of their hydraulic phases $C_4A_3\overline{S}$, CA (CSA-1 only) and C_2S (CSA-2 only) obtained from XRD. In order to reflect the Si concentrations in the pore solution of CSA-1, a small amount (0.2 wt.%) of gehlenite was allowed to dissolve. Gypsum in CSA-1 was regarded to be readily soluble, whereas a dissolution kinetics for the anhydrite in CSA-2 based on XRD intensities was applied. The alkalis present in the cements were partly regarded as readily soluble and partly distributed between the different solid phases by fitting the dissolution kinetics of the anhydrous phases with the pore solution data. Siliceous hydrogarnets, which should occur as a stable hydrate phase not only in CSA cements, but also in ordinary Portland cement, were not allowed to precipitate, as this is not in agreement with the experimental findings. At room temperature their formation is very slowly [37]. Also the formation of gibbsite instead of amorphous $Al(OH)_3$ and the formation of CAH_{10} were inhibited for the same reasons.

Fig. 8 shows the thermodynamic modelling of the phase development (phase content in g per 100 g dry cement) of CSA-1 and CSA-2 pastes with ongoing hydration. In the CSA-1 paste, the dissolution of ye'elimite and calcium aluminate leads during the first 8 h to a continuous consumption of gypsum. As hydrate phases ettringite and amorphous $Al(OH)_3$ form, and the amount of pore solution decreases. After 8 h the gypsum is depleted, and thus ettringite formation stops. Instead, monosulfate now forms together with amorphous $Al(OH)_3$. The reaction of ye'elimite to monosulfate results in a higher rate of $Al(OH)_3$ formation compared to the reaction of ye'elimite with gypsum to ettringite. After 28 days, ettringite is the main hydration product; it is accompanied by $Al(OH)_3$ and monosulfate as minor hydrate phases. Strätlingite forms only in low amounts, as just a small quantity of gehlenite was allowed to dissolve based on the experimental observations. The experimental amount of pore solution, ettringite and gypsum (in the case of CSA-1) amount derived from TGA show a very good agreement with the corresponding values obtained from the thermodynamic modelling. The modelled phase development also correlates very well with the experimental findings by XRD and TGA.

In CSA-2, ye'elimite, belite and anhydrite are dissolving with time. In contrast to the gypsum in CSA-1, a dissolution kinetics was assigned to the anhydrite. Thus, it is not consumed after 28 days of hydration. The dissolution of the above mentioned phases leads to the formation of ettringite, amorphous $Al(OH)_3$ and strätlingite, while the quantity of pore solution decreases. Monosulfate forms only after about 2 days of hydration, when the main part of ye'elimite and anhydrite has already dissolved. At this time, also the formation of $Al(OH)_3$ stops, and its amount decreases slightly while more strätlingite is formed. After 28 days, ettringite and strätlingite are the main hydration products, $Al(OH)_3$ and monosulfate are minor products. Also in the case of CSA-2, the results of the thermodynamic modelling agree very well with the experimental values.

With the densities of all phases present, the development of the individual phase volumes as well as the total volume can be calculated, as shown in Fig. 9. The hydration leads to an increase of

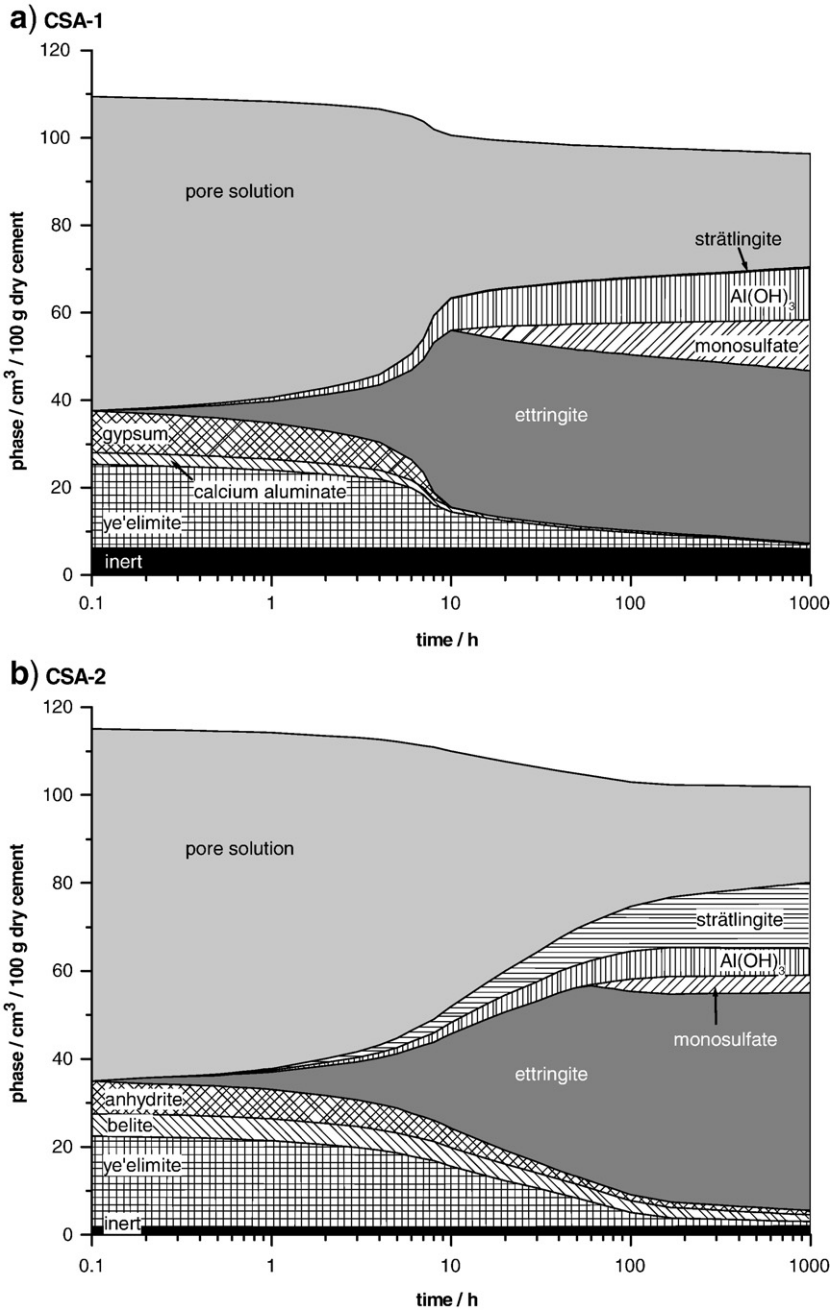

Fig. 9. Modelled changes of phase volumes during hydration of a) CSA-1 and b) CSA-2.

the volume of solids and to a decrease of the volume of the liquid phase. For both CSA cements, the total volume decreases with time, reflecting a calculated chemical shrinkage of 11.4 cm^3/100 g dry cement (CSA-1) and 11.5 cm^3/100 g dry cement (CSA-2) after 28 days. These values are higher than those measured for an ordinary Portland cement, see e.g. [45], of about 4–5 cm^3/100 g dry cement after 28 days of hydration. For both cements ettringite makes the main contribution to the volume of the hydrated paste.

5. Conclusions

In this study the hydration mechanisms of two calcium sulfoaluminate cements have been investigated by experimental means as well as by thermodynamic modelling. During the first hours of hydration, ettringite and amorphous $Al(OH)_3$ form from the hydration of ye'elimite. After the depletion of the calcium sulfate, monosulfate starts to occurs together with a strong decrease of Ca and sulfate concentrations in the pore solution and an increase of pH from about 10–11 to 12.5–12.8.

If belite is present as minor phase, strätlingite forms as further hydration product, consuming a part of the amorphous $Al(OH)_3$. The formation of C–S–H phases was not observed experimentally and is also unlikely as they are undersaturated with respect to the ionic composition of the liquid phase. The silica dissolved is instead incorporated into strätlingite, which is oversaturated throughout the whole investigated hydration period. As other authors report the presence of C–S–H in CSA cements, which could not be confirmed in the case of the belite containing CSA-2, further investigations are needed concerning the stabilities of strätlingite and C–S–H in systems like hydrated CSA cements without available portlandite and calcium sulfate.

The microstructure of CSA-2 appears more inhomogeneously compared to CSA-1 with large amounts of big strätlingite crystals

present after 28 days. Pore solution analysis revealed as well that strätlingite acts as a sink for the potassium released from the hydrating clinker phases.

The two types of calcium sulfate in CSA-1 and CSA-2 behave differently. The analysis of the pore solution shows in the case of CSA-1 that it is saturated with respect to gypsum until the gypsum is depleted after 16 h of hydration. The anhydrite in CSA-2 is undersaturated beyond 1 h of hydration due to its slower dissolution kinetics compared to the gypsum. This emphasizes that a reactive calcium sulfate able to provide enough calcium and sulfate ions is crucial to control the hydration of CSA cements.

The thermodynamic model developed in this study can be used to predict the hydration of CSA cements, allowing an easy and fast parameter variation like clinker composition, amount of calcium sulfate or water/cement ratio.

Acknowledgements

The authors express their thanks to Boris Ingold and Luigi Brunetti (Empa, Laboratory for Concrete and Construction Chemistry), as well as to Herrmann Mönch (Eawag, Department Water Resources and Drinking Water) for their help with the experimental part of the work.

References

[1] E. Gartner, Industrially interesting approaches to "low-CO_2" cements, Cem. Concr. Res. 34 (9) (2004) 1489–1498.
[2] J.S. Damtoft, J. Lukasik, D. Herfort, D. Sorrentino, E.M. Gartner, Sustainable development and climate change initiatives, Cem. Concr. Res. 38 (2) (2008) 115–127.
[3] M. Su, W. Kurdowski, F. Sorrentino, Development in non-Portland cements, 9th International Congress on the Chemistry of Cements, New Delhi, India, I, Nov. 23–28, 1992, pp. 317–354.
[4] J.H. Sharp, C.D. Lawrence, R. Yang, Calcium sulfoaluminate cements — low-energy cements, special cements or what? Adv. Cem. Res. 11 (1) (1999) 3–13.
[5] F.P. Glasser, L. Zhang, High-performance cement matrices based on calcium sulfoaluminate-belite compositions, Cem. Concr. Res. 21 (12) (2001) 1881–1886.
[6] M. Su, J. Deng, Z. Wu, X. Liu, Research on the chemical composition and microstructures of sulpho-aluminate cement clinker, 9th International Congress on the Chemistry of Cements, New Delhi, India, II, Nov. 23–28, 1992, pp. 94–100.
[7] M.M. Ali, S. Gopal, S.K. Handoo, Studies on the formation kinetics of calcium sulphoaluminate, Cem. Concr. Res. 24 (4) (1994) 715–720.
[8] S. Sahu, J. Majling, Phase compatibility in the system $CaO–SiO_2–Al_2O_3–Fe_2O_3–SO_3$ referred to sulphoaluminate belite cement clinker, Cem. Concr. Res. 23 (6) (1993) 1331–1339.
[9] J. Beretka, B. de Vito, L. Santoro, N. Sherman, G.L. Valenti, Hydraulic behaviour of calcium sulfoaluminate-based cements derived from industrial process wastes, Cem. Concr. Res. 23 (5) (1993) 1205–1214.
[10] S. Sahu, J. Majling, Preparation of sulphoaluminate belite cement from fly ash, Cem. Concr. Res. 24 (6) (1994) 1065–1072.
[11] P. Arjunan, M.R. Silsbee, D.M. Roy, Sulfoaluminate-belite cement from low-calcium fly ash and sulfur rich and other industrial by-products, Cem. Concr. Res. 29 (8) (1999) 1305–1311.
[12] S. Sahu, J. Havlica, V. Tomková, J. Majling, Hydration behaviour of sulphoaluminate belite cement in the presence of various calcium sulphates, Thermochim. Acta 175 (1) (1991) 45–52.
[13] J. Péra, J. Ambroise, E. Holard, G. Beauvent, Influence of the type of calcium sulfate on the properties of calcium sulfoaluminate cemen, 11th International Congress on the Chemistry of Cements, Durban, South Africa, 3, May 11–16, 2003, pp. 1129–1135.
[14] G. Bernardo, A. Telesca, G.L. Valenti, A porosimetric study of calcium sulfoaluminate cement pastes cured at early ages, Cem. Concr. Res. 36 (6) (2006) 1042–1047.
[15] L. Zhang, F.P. Glasser, Hydration of calcium sulfoaluminate cement at less than 24 h, Adv. Cem. Res. 14 (4) (2002) 141–155.
[16] M. Andac, F.P. Glasser, Pore solution composition of calcium sulfoaluminate cement, Adv. Cem. Res. 11 (1) (1999) 23–26.
[17] L. Zhang, F.P. Glasser, Investigation of the microstructure and carbonation of $C\overline{S}A$-based concretes removed from service, Cem. Concr. Res. 35 (12) (2005) 2252–2260.
[18] G.S. Li, G. Walenta, E.M. Gartner, Formation and hydration of low CO_2 cements based on belite, calcium sulfoaluminate and calcium aluminoferrite, 12th International Congress on the Chemistry of Cement, Montreal, Canada, paper TH3-15.3, July 8–13, 2007, 12 pp.
[19] A. Alaoui, H. Nguyen, L. Divet, A. Feraille, R. Le Roy, Experimental studies of hydration mechanisms of sulfoaluminate clinker, 12th International Congress on the Chemistry of Cement, Montreal, Canada,, paper W3–11.6, July 8–13, 2007, 12 pp.
[20] N. Sherman, J. Beretka, L. Santoro, G.L. Valenti, Long-term behaviour of hydraulic binders based on calcium sulfoaluminate and calcium sulfosilicate, Cem. Concr. Res. 25 (1) (1995) 113–126.
[21] K. Quillin, Performance of belite-sulfoaluminate cements, Cem. Concr. Res. 31 (9) (2001) 1341–1349.
[22] I. Janotka, L. Krajči, An experimental study on the upgrade of sulfoaluminate-belite cement systems by blending with Portland cement, Adv. Cem. Res. 11 (1) (1999) 35–41.
[23] I. Janotka, L. Krajči, A. Ray, S.C. Mojumdar, The hydration phase and pore structure formation in the blends of sulfoaluminate–belite cement with Portland cement, Cem. Concr. Res. 33 (4) (2003) 489–497.
[24] J. Péra, J. Ambroise, New applications of calcium sulfoaluminate cements, Cem. Concr. Res. 34 (4) (2004) 671–676.
[25] J.F. Georgin, J. Ambroise, J. Péra, J.M. Reynouard, Development of self-leveling screed based on calcium sulfoaluminate cement: modelling of curling due to drying, Cem. Concr. Compos. 30 (9) (2008) 769–778.
[26] V. Albino, R. Cioffi, M. Marroccoli, L. Santoro, Potential application of ettringite generating systems for hazardous waste stabilization, J. Hazard. Mater. 51 (1–3) (1996) 241–252.
[27] S. Peysson, J. Péra, M. Chabannet, Immobilization of heavy metals by calcium sulfoaluminate cement, Cem. Concr. Res. 35 (12) (2005) 2261–2270.
[28] C.A. Luz, J.C. Rocha, M. Cheriaf, J. Péra, Use of sulfoaluminate cement and bottom ash in the solidification/stabilization of galvanic sludge, J. Hazard. Mater. 136 (3) (2006) 837–845.
[29] Q. Zhou, N.B. Milestone, M. Hayes, An alternative to Portland cement for waste encapsulation — the calcium sulfoaluminate cement system, J. Hazard. Mater. 136 (1) (2006) 120–129.
[30] C.A. Luz, J. Pera, M. Cheriaf, J.C. Rocha, Behaviour of calcium sulfoaluminate cement in presence of high concentrations of chromium salts, Cem. Concr. Res. 37 (4) (2007) 624–629.
[31] available at http://gems.web.psi.ch.
[32] V.I. Babushkin, G.M. Matveyev, O.P. Mchedlov-Petrossyan, Thermodynamics of Silicates, Springer-Verlag, Berlin, 1985.
[33] W. Hummel, U. Berner, E. Curti, F.J. Pearson, T. Thoenen, , Nagra/PSI Chemical Thermodynamic Data Base 01/01, Universal Publishers/uPUBLISH.com, USA, Also Published as Nagra Technical Report NTB 02-16, Wettingen, Switzerland, 2002.
[34] T. Thoenen, D. Kulik, Nagra/PSI Chemical Thermodynamic Database 01/01 for the GEM-Selektor (V.2-PSI) Geochemical Modeling Code, PSI, Villigen, 2003, available at http://les.web.psi.ch/Software/GEMSPSI/doc/pdf/TM-44-03-04-web.pdf.
[35] B. Lothenbach, F. Winnefeld, Thermodynamic modelling of the hydration of Portland cement, Cem. Concr. Res. 36 (2) (2006) 209–226.
[36] T. Matschei, B. Lothenbach, F.P. Glasser, Thermodynamic properties of Portland cement hydrates in the system $CaO–Al_2O_3–SiO_2–CaSO_4–CaCO_3–H_2O$, Cem. Concr. Res. 37 (10) (2007) 1379–1410.
[37] B. Lothenbach, T. Matschei, G. Möschner, F.P. Glasser, Thermodynamic modelling of the effect of temperature on the hydration and porosity of Portland cement, Cem. Concr. Res. 38 (1) (2008) 1–18.
[38] available at http://www.empa.ch/cemdata, Version cemdata07.2, release date 14.08.08
[39] B. Lothenbach, E. Wieland, A thermodynamic approach to the hydration of sulphate-resisting Portland cement, Waste Manage. 26 (7) (2006) 706–719.
[40] B. Lothenbach, G. Le Saout, E. Gallucci, K. Scrivener, Influence of limestone on the hydration of Portland cements, Cem. Concr. Res. 38 (6) (2008) 848–860.
[41] B. Lothenbach, A. Gruskovnjak, Hydration of alkali-activated slag: thermodynamic modelling, Adv. Cem. Res. 19 (2) (2007) 81–92.
[42] A. Gruskovnjak, B. Lothenbach, F. Winnefeld, R. Figi, S.-C. Ko, M. Adler, U. Mäder, Hydration mechanisms of super sulphated slag cements, Cem. Concr. Res. 38 (7) (2008) 983–992.
[43] R.S. Barneyback, S. Diamond, Expression and analysis of pore fluids from hardened cement pastes and mortars, Cem. Concr. Res. 11 (2) (1981) 279–285.
[44] D. Damidot, F.P. Glasser, Investigation of the $CaO–Al_2O_3–SiO_2–H_2O$ system at 25 °C by thermodynamic calculations, Cem. Concr. Res. 25 (1) (1995) 22–28.
[45] M. Geiker, T. Knudsen, Chemical shrinkage of Portland cement pastes, Cem. Concr. Res. 12 (5) (1982) 603–610.